

Purdue University Purdue e-Pubs

International Compressor Engineering Conference

School of Mechanical Engineering

2018

A Novel Structure of Rolling Piston Type Rotary Compressor

Myeong Su Shin

Graduated School of Smart Interdisciplinary Engineering, Pusan National University, Busan, 609-735, Korea,
shinms7@pusan.ac.kr

Sang-kyung Na

Graduate School of Mechanical Engineering, Pusan National University, Busan, Republic of (South Korea),
naskng@pusan.ac.kr

G.M. Choi

Pusan National University, choigm@pusan.ac.kr

Follow this and additional works at: <https://docs.lib.purdue.edu/icec>

Shin, Myeong Su; Na, Sang-kyung; and Choi, G.M., "A Novel Structure of Rolling Piston Type Rotary Compressor" (2018).
International Compressor Engineering Conference. Paper 2595.
<https://docs.lib.purdue.edu/icec/2595>

This document has been made available through Purdue e-Pubs, a service of the Purdue University Libraries. Please contact epubs@purdue.edu for additional information.

Complete proceedings may be acquired in print and on CD-ROM directly from the Ray W. Herrick Laboratories at <https://engineering.purdue.edu/Herrick/Events/orderlit.html>

A Novel Structure of Rolling Piston Type Rotary Compressor

Myeong Su Shin¹, Sang Kyung Na², Gyung Min Choi^{3*}

¹Graduated School of Smart Interdisciplinary Engineering, Pusan National University, Busan, Korea
(E-mail : shinms7@pusan.ac.kr)

²Graduated School of Mechanical Engineering, Pusan National University, Busan, Korea
(E-mail : naskng@pusan.ac.kr)

³Department of Mechanical Engineering, Pusan National University, Busan, Korea
(E-mail : choigm@pusan.ac.kr)

* Corresponding Author

ABSTRACT

This paper presents a new design of rolling piston type rotary compressor and the analysis of the performance of the novel compressor is conducted. The concept of the novel compressor is to utilize the interior space of the roller as inner working volume. The vane is connected and fixed to the outer cylinder and the inner cylinder, and the split bush is located between the roller and the vane to help revolution of the roller. Therefore, the novel compressor has two working volumes. One is outer volume trapped within the outer cylinder, the vane, and the roller and the other is inner volume trapped within the inner cylinder, the vane, and the roller. In the same frame size, the cooling capacity of the novel compressor is increased by average 34.77% over that of the traditional rolling piston type rotary compressor. This is because the mass flow rate of the refrigerant into the compressor increases due to the increase of the total working volume. However, the input power is also increased by average 23.4% over that of the traditional rolling piston type rotary compressor. It is because the indicated work increases due to inner compression work. As a result, the energy efficiency ratio (EER) of the novel compressor is increased by 9.42% over that of the traditional rolling piston type compressor.

1. INTRODUCTION

Due to the environmental concerns, there is a growing demand for high efficiency systems in recent years. In the refrigeration system, most of the power consumption of the entire system is used in the compressor. In this reason, the researches on the optimization of the structure of compressors have been conducted to improve the performance of the compressors. The rotary type compressors have been widely used in household and industrial refrigeration system because of their advantages such reliability, continuous supply of refrigerant, miniaturization, and so on. Tan and Ooi (2011) presented design improvements of a Revolving Vane (RV) compressor which significantly reduce the frictional losses by rigidly fixing the vane onto the rotor or the cylinder. As a result, the friction losses decrease by 17% and 41%, respectively. The mechanical efficiency is improved by 93% to 94% and 96%, respectively. Bradshaw and Groll (2013) studied on the simulation model of a novel rotating spool compressor. Liu *et al.* (2016) suggested the new injection structure on the blade of a rotary compressor. By placing the injection channel in the vane, it can eliminate the back-flowing of the injected refrigerant. The new injection structure can be improved volume efficiency and mass flow rate by 1.8% to 2.7% and 26.6% to 57.2%, respectively, compared to traditional injection structure. Also, the heating capacity and coefficient of performance (COP) increase by 23.1% to 48.9% and 3.2% to 8.0%, respectively. Yang and Qu (2017) presented a novel double-swing vane compressor (DSVC) for use in electric vehicle air conditioning systems. The theoretical volumetric flow rate of the DSVC is about 1.6 times that of the swing vane compressor (SVC) with a single swing vane. They presented that the lower vanes induce additional friction losses, but the mechanical efficiency of the DSVC is higher than the mechanical efficiency of the SVC under the same operating conditions and dimensions. Moreover, they presented that the loading conditions on the eccentric and shaft bearings in the DSVC are relatively better than those in the SVC due to the smaller fluctuations in the pressure forces.

Yap *et al.* (2018) introduced the novel cross vane expander-compressor (CVEC). This device amalgamates of the compressor and expander into a single unit, permitting fluid compression and expansion energy recovery to be accomplished simultaneously. Therefore, the proposed CVEC system improves the overall COP by 36.6% as compared to that of the basic vapor compression system. In this paper, a novel structure of the rolling piston type compressor for high efficiency and compactable is introduced. The novel compressor is analyzed through numerical models and compare the performance of the compressor with traditional rolling piston type compressor.

2. DESIGN AND WORKING PRINCIPLE

2.1 Design

Fig. 1 shows the difference in structure between the traditional rolling piston type (RP) compressor and the proposed compressor in this paper. The RP compressor has only one working volume, however, the novel compressor has two working volumes by utilizing the internal space. As shown in Fig. 1(b), there is a difference in height between the outer cylinder and the inner cylinder because of the eccentric part height and the power is transmitted from the eccentric part to the roller side plate. The vane connects the outer cylinder to the inner cylinder and separates the suction chamber and the compression chamber in the stroke volumes. The outer and inner strokes have a phase difference of 180° because of structural feature.

2.2 Working principle

Fig. 2 shows the schematic of the working principle of the novel compressor. It shows every 90° when the shaft rotates counterclockwise. The suction and compression processes begin in the inner suction and compression chamber,

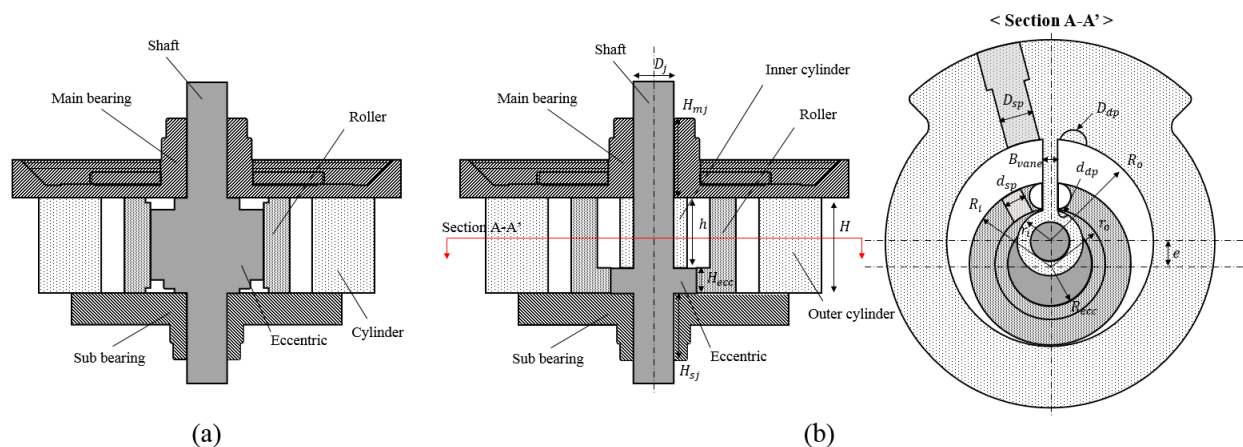


Figure 1 : Comparison (a) traditional rolling piston type compressor and (b) the novel compressor

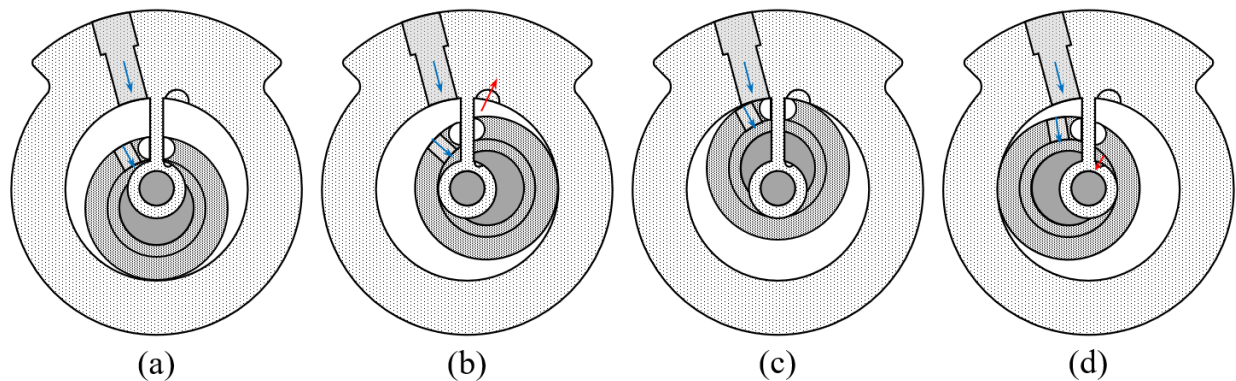


Figure 2 : Working process of the novel compressor

respectively (Fig. 2a). The gas in the inner chamber flows from the outer chamber through the suction pipe located in the roller. At the same time, the suction and compression strokes at outer chamber have already proceeded by half a stroke. As the shaft rotates, the pressure in the outer compression chamber becomes higher than the discharge pressure and the discharge process starts (Fig. 2b). Hereafter, the discharge process at outer compression chamber finishes (Fig. 2c) and the discharge process at inner compression chamber starts (Fig. 2d).

3. NUMERICAL MODELING

The definition of the control volume is needed before the analysis of the compressor performance. Fig. 3 shows the control volumes for numerical analysis of the novel compressor and main flow between control volumes. The novel compressor is divided into 13 control volumes, and the properties are calculated from each control volume such as volume, density, temperature, and pressure.

3.1 Geometric model

The volumes of the outer and inner chamber are changed with the rotation angle as follows,

$$V_{o,suc} = \frac{1}{2}H[(e + R_i)^2\theta - R_i^2(\theta + \alpha_{out}) - e\sin\theta(e \cos \theta + R_i \cos \alpha_{out}) - B_{vane}ext_{out}] \quad (1)$$

$$V_{i,suc} = \frac{1}{2}h[r_o^2(\theta - \alpha_{in}) + r_i^2\theta + e \sin \theta (r_o \cos \alpha_{in} - e \cos \theta) + B_{vane}ext_{in}] \quad (2)$$

$$V_{o,comp} = \frac{\pi}{4}(R_o^2 - R_i^2)H - V_{o,suc}, \quad V_{i,comp} = \frac{\pi}{4}(r_o^2 - r_i^2)h - V_{i,suc} \quad (3)$$

Where,

$$ext_{out} = R_o - (e \cos \theta + R_i \cos \alpha_{out}), \quad ext_{in} = r_o \cos \alpha_{in} - e \cos \theta - r_i \quad (4)$$

$$\alpha_{out} = \sin^{-1}\left(\frac{e \sin \theta}{R_i}\right), \quad \alpha_{in} = \sin^{-1}\left(\frac{e \sin \theta}{r_o}\right) \quad (5)$$

3.2 Leakage model

In the novel compressor, leakage occurs between the vane bush and the vane, roller surface, radial clearance, and crankshaft. Actually, the leakage is calculated by many variables such as the pressure difference, flow area, shape of

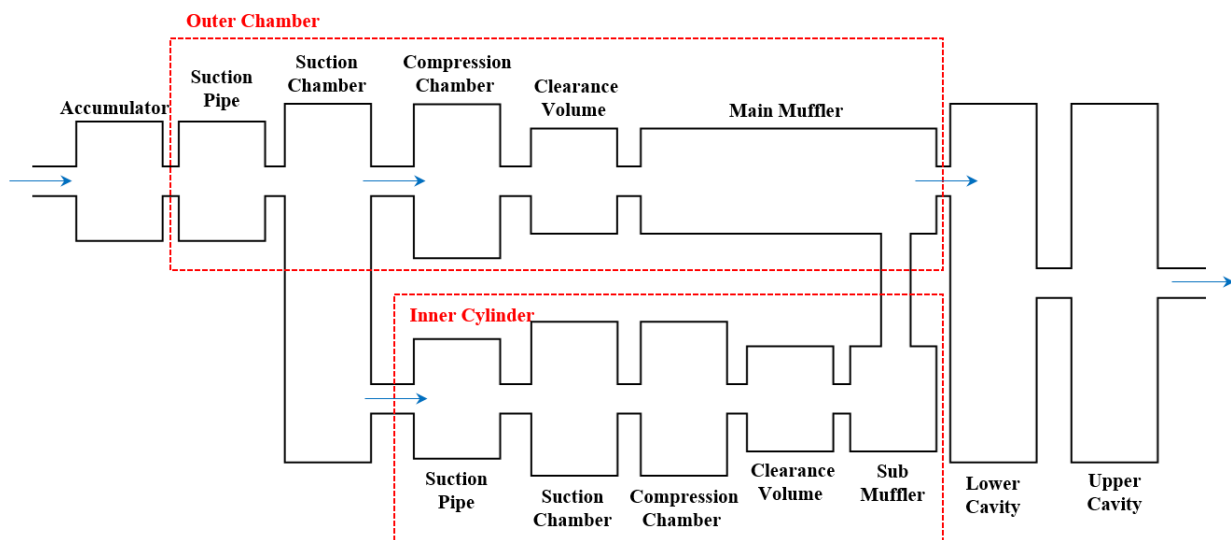


Figure 3 : Definition of the control volumes

the flow path, and so on. Generally, the leakage is calculated through some assumption in the simulation because all the influenced factor cannot be considered. The leakage is one-dimensional compressible isentropic flow, ignoring kinetic energy and friction effects on flow, and is considered a simple orifice flow. The leakage is calculated by follows,

$$P_{cr} = \left(\frac{2}{k+1} \right)^{\frac{k}{k-1}} \quad (6)$$

For $P_{cr} < P_d/P_u$

$$\dot{m} = C_v P_u A \sqrt{\frac{2k}{(k-1)RT_u} \left[\left(\frac{P_d}{P_u} \right)^{\frac{2}{k}} - \left(\frac{P_d}{P_u} \right)^{\frac{k+1}{k}} \right]} \quad (7)$$

For $P_{cr} \geq P_d/P_u$

$$\dot{m} = C_v P_u A \sqrt{\frac{k}{RT_u} \left(\frac{2}{k+1} \right)^{\frac{k+1}{2(k-1)}}} \quad (8)$$

Where, P_{cr} is critical pressure ratio. When critical pressure ratio is less than the pressure ratio of downstream to upstream, the leakage is calculated by Eq. (7). However, if critical pressure ratio is greater than or equal to the pressure ratio of downstream to upstream, the leakage is calculated by Eq. (8). It is called choked flow.

3.3 Dynamic model

Fig. 4 shows the forces and moments acting on the roller and the shaft. The mechanical loss of the novel compressor is obtained through the force and moment equilibrium equations and is consist of 7 parts. Table 1 shows the type of the mechanical loss and its equation.

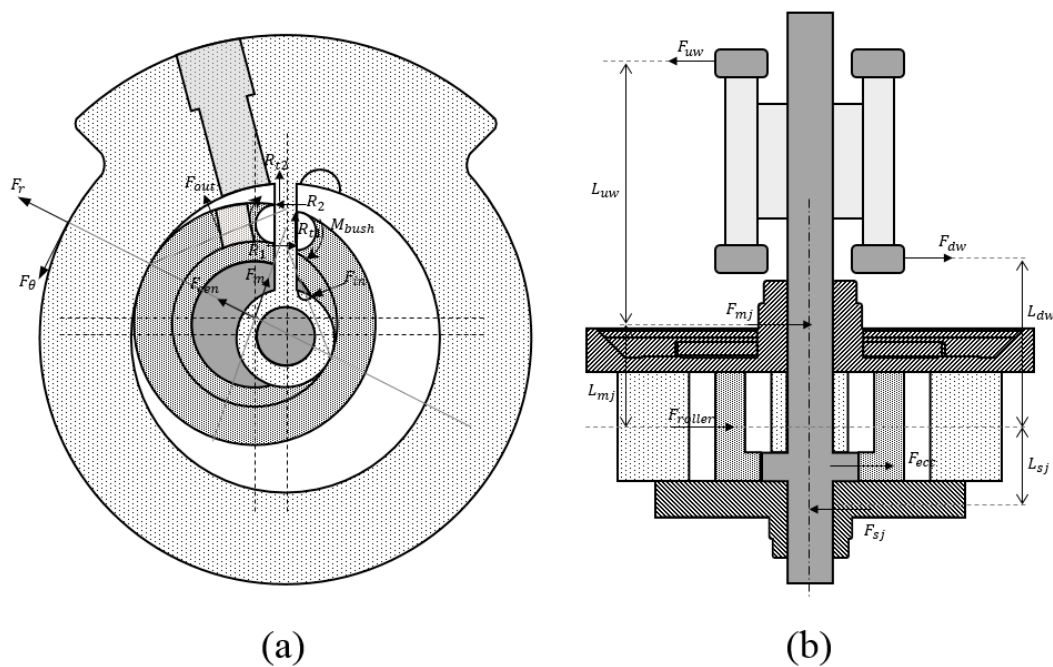


Figure 4 : Forces and moments acting on (a) the roller and (b) the crank shaft

Table 1 : Mechanical losses of the novel compressor

Nomenclature	Sliding surface	Equation
L_s	Vane/Vane bush	$ (R_{t1} + R_{t2})\dot{\gamma} $
L_{bush}	Roller/Vane bush	$M_{bush} \dot{\alpha} $
L_b	Roller/Cylinder	$M_b\omega_p$
L_c	Roller/Eccentric	$ \omega - \omega_p M_c$
L_{mj}	Main journal bearing	$\omega r_j f_{mj} F_{mj}$
L_{sj}	Sub journal bearing	$\omega r_j f_{sj} F_{sj}$
L_{tb}	Thrust surface	$\omega r_{tb} f_{tb} F_{tb}$

3.4 Performance indicators

The performance of the novel compressor can be indicated by cooling capacity (Q_c), input power of the compressor (W_c), and energy efficiency ratio (EER). The cooling capacity can be obtained by discharge mass flow rate and the enthalpy difference between the evaporator inlet and outlet.

$$Q_c = \dot{m}_{dis}(h_{eva,out} - h_{eva,in}) \quad (9)$$

The input power of the compressor (W_c) can be obtained by indicated work (W_{indi}), mechanical loss (L_{mech}), and motor efficiency (η_{motor}).

$$W_c = \frac{W_{indi} + L_{mech}}{\eta_{motor}} \quad (10)$$

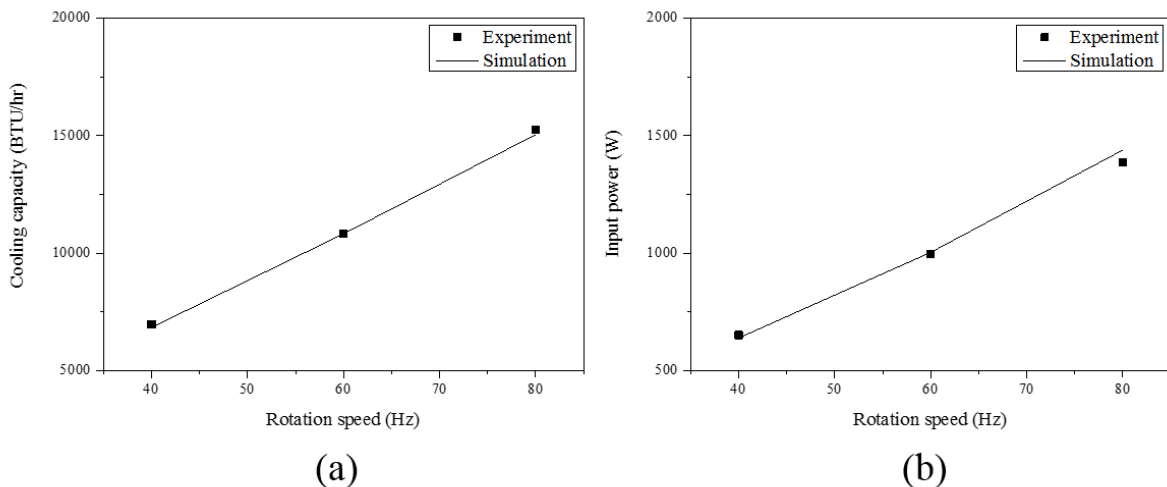
Where, mechanical loss (L_{mech}) is sum of all of the mechanical loss.

$$L_{mech} = L_s + L_{bush} + L_c + L_{mj} + L_{sj} + L_{tb} \quad (11)$$

5. RESULT AND DISCUSION

5.1 Validation of the simulation

Fig. 5 shows experimental and simulation results of RP compressors with operating conditions (P_s : 10.15 bar, P_d : 34.48 bar, rotation speed : 40 ~ 80 Hz). As shown in Fig. 5, the maximum errors of the cooling capacity and input

**Figure 5** : Comparison experimental and simulation results of RP compressor

power of RP compressor are 2.0% and 3.66%, respectively. Therefore, the numerical analysis model used for the compressor analysis is reliable. In the case of the novel compressor, the same numerical analysis model as that of the RP compressor is used. In this paper, the analysis of the novel compressor with the same frame size as the RP compressor is conducted.

5.2 Compressor performance analysis

The compressor performance analysis is conducted under high pressure ratio condition ($P_s : 10.15 \text{ bar}$, $P_d : 34.48 \text{ bar}$) and low pressure ratio condition ($P_s : 10.15 \text{ bar}$, $P_d : 23.37 \text{ bar}$) with variation of the rotation speed. Fig. 6 shows the pressure-volume diagram of the outer chamber (a) and the inner chamber (b) under high pressure ratio condition and 60Hz. According Fig. 6, the suction loss of the inner chamber is larger than that of the outer chamber. It is because the flow resistance is large due to the structure characteristic that the gas flowing into the inner chamber flows thorough pass the outer chamber. In addition, the maximum pressure and the over compression loss of the inner chamber are larger than that of the outer chamber. It is because the discharge port size of the inner chamber is smaller than that of the outer chamber and the discharge speed of the gas is slow. Fig. 7 shows the performance of the novel compressor under the high and low pressure ratio with variation of the rotation speed. As shown Fig. 7, EER of the RP compressor and the novel compressor are 70.15% and 74.19% higher than at the high pressure ratio at the low pressure ratio condition. Compared to the RP compressor and the novel compressor, the cooling capacity and the input power of the novel compressor increase by 34.77% and 23.40%, respectively. As a result, EER of the novel compressor increases by 9.42%.

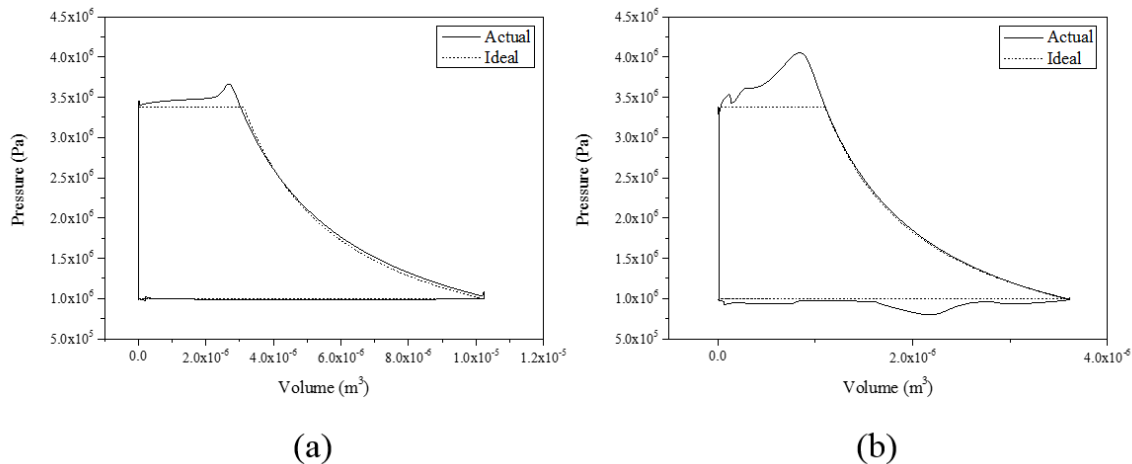


Figure 6 : Pressure and volume diagram at the outer chamber (a) and the inner chamber (b)

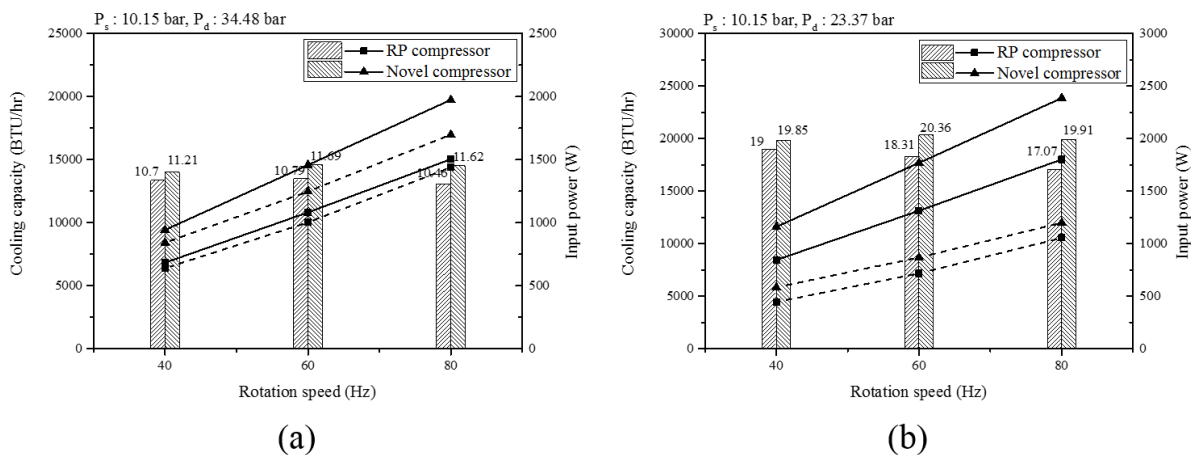


Figure 7 : Comparison performance of the RP compressor and the novel compressor

6. CONCLUSIONS

In this paper, a new structure of the rolling piston type compressor is proposed. The purpose of the novel structure is to miniaturize the compressor size and improve the performance of the compressor by securing the eccentric space in the RP compressor. The performance analysis of the RP compressor and the novel compressor is conducted and the performance of these compressors are compared. The results are summarized as follows:

- The cooling capacity of the novel compressor is increased by 34.77%.
- The input power of the novel compressor is also increased by 23.40%
- EER of the novel compressor is increased by 9.42%.

NOMENCLATURE

B	width	(m)
D	diameter (outer cylinder)	(m)
d	diameter (inner cylinder)	(m)
e	eccentricity	(m)
ext	vane extrusion length	(m)
F	force	(N)
H	height (outer cylinder)	(m)
h	height (inner cylinder)	(m)
k	specific heat ratio	
P	pressure	(Pa)
R	radius (outer cylinder)	(m)
r	radius (inner cylinder)	(m)
V	volume	(m ³)
Θ	rotation angle (outer cylinder)	(degree)
θ	rotation angle (inner cylinder)	(degree)

Subscript

suc	suction chamber
comp	compression chamber
mj	main journal bearing
sj	sub journal bearing
sp	suction pipe
ecc	eccentric part
i	inner
o	outer
u	upstream
d	downstream
dis	discharge
eva	evaporator

REFERENCES

- Bradshaw, C. R. & Groll, E. A. (2013). A comprehensive model of a novel rotating spool compressor. *Int. J. Refrig.*, 36(7), 1974-1981.
- Liu, X., Wang, B., Shi, W. & Zhang, P. (2016). A novel vapor injection structure on the blade of a rotary compressor. *Appl. Therm. Eng.*, 100, 1219-1228.
- Tan, K. M. & Ooi, K. T. (2011). A novel revolving vane compressor with a fixed-vane. *Int. J. Refrig.*, 34(8), 1980-1988.
- Yang, X., Dong, C. & Qu, Z. (2017). Design and dynamic analysis of a novel double-swing vane compressor for electric vehicle air conditioning systems. *Int. J. Refrig.*, 76, 52-62.
- Yap, K. S., Ooi, Kim Tiow & Chakraborty A. (2018). Analysis of the novel cross vane expander-compressor: Mathematical modelling and experimental study. *Energy*, 145, 626-637.

ACKNOWLEDGEMENT

This work was supported by “Human Resources Program in Energy Technology” of the Korea Institute of Energy Technology Evaluation and Planning (KETEP), granted financial resource from the Ministry of Trade, Industry & Energy, Republic of Korea. (No. 20164010201000)